How to map the Gravitational Wave background of the primordial universe

Identifying key technical challenges

Luka W. Bowen

July 2023

Abstract

This paper introduces our novel idea of using the Sun as a gravitational lens to detect the primordial gravitational wave background. Our objective is to advance the current understanding of the universe, its formation, early events, and inflation, which we are currently unable to describe or observe.

The research comprises of two main components: a simulation to understand the Sun's lensing effect on gravitational waves and a proof-of-concept machine learning algorithm that can reverse this lensing effect. The simulation models the Sun's lensing effect on different objects at varying distances. Our approach is simplified compared to the intricate simulations found in literature, with the focus being on structured objects such as letters and symbols to demonstrate the lensing effect more clearly. The machine learning algorithm, trained on this simulated data, shows promising results in its ability to learn the Sun's lensing effect and reconstruct the original images.

Further, we delve into the feasibility and cost of operating a hypothetical gravitational wave detector, estimated based on costs associated with similar space missions. The study lays out a road-map for future work in improving the simulations, refining the machine learning model, and investigating practical considerations for using the Sun as a gravitational lens.

Our results open up avenues for exploring the detection of primordial gravitational waves, and provide a strong foundation for future research in gravitational imaging, the creation of AI collimators and the use of Sun for cosmological observations.

1 Introduction

1.1 CMB Discovery

The discovery of the Cosmic Microwave Background (CMB) by Penzias and Wilson [1], and the first images taken by the COBE satellite [2], provided strong evidence in support of the Big Bang Theory and changed our understanding of the universe. The CMB gives us a clear picture of the universe approximately 380,000 years after the Big Bang. At this time, the universe had cooled down enough for atoms to form; as these atoms formed, the number of free electrons in the universe decreased. The decrease in electrons meant that photons stopped being scattered and were able to travel freely throughout the universe. However, minute fluctuations in temperature caused variations in homogeneity, which amount to less than 1/10,000 of the photon emission. These variations can be measured and mapped out across the universe. These temperature fluctuations correspond to different energy densities at the time the CMB was formed, giving a snapshot of what the universe looked like at this time.

The first image of the CMB was very low resolution, not providing much detail. Despite this, it was still considered an astonishing achievement for the time, as it was the first time the inhomogeneity of the CMB was experimentally verified. Over time, as more sensitive measurement techniques were developed, such as those used by the WMAP [3], PLANCK [4], and other instruments, clearer images were obtained. These advanced images allow us to read the CMB in more detail and improve existing theories.

While the CMB provides evidence supporting some theories on the formation of the universe, such as cosmic inflation [5], ongoing research is still needed to fully interpret the information contained within the CMB. For instance, recent studies have focused on the B-modes in the CMB, a type of polarization that, if detected, could provide evidence of gravitational waves from the early universe [6].

The main restriction of the CMB is the moment of its formation; we cannot observe anything in the universe before it, it would be interesting to be able to observe the universe before these moments.

1.2 Gravitational Waves as a means to peek further into the past

Recent theories and research efforts explore potential ways to glean information about the universe almost instantly after its formation, such as through the study of gravitational waves [7]. Being able to do this would be of the utmost importance as it would allow us to observe almost every cosmological and physical event since the beginning of the universe, and luckily there may be an answer. Gravitational waves, which are ripples in space-time are interesting phenomena as they, unlike photons were free to travel to the opaque universe. It is hypothesized that early cosmological events, such as cosmic inflation, symmetry violations, field separations all caused gravitational waves to be created. If

we were able to observe these primordial gravitational waves, as we are photons in the CMB, it would provide an answer to our question.

Gravitational waves were first predicted by Einstein in 1916 [10]. The effect is extremely weak (The coupling parameter is 10^{-43}), therefore even Einstein himself thought it was immeasurable [11]. It took until 2015 before they were first detected by the LIGO consortium [7].

The *Gravitational Wave Background* (GWB) is a stochastic background comprised of the gravitational waves formed in the early universe according to the Lambda-CDM model [12]. As stated earlier, each significant event starting 10^{-36} seconds after the Big Bang would be recorded within the GWB. This would provide us with unparalleled insight into the early universe and enable us to validate or falsify current cosmological theories. It is also important to note, the GWB is a cumulative map, meaning that it is not a snapshot of the universe at a given moment, but instead a cumulative history of the entire universe up to today.

Unlike photons, gravitational waves are not easy to observe. Even the most violent events in the universe, such as black hole collisions, create waves which we detect with an amplitude of about 10 Hz. It is expected that primordial gravitational waves would have an frequency of about 10^{-6} Hz, which presents a significant challenge for our current detection methods that are simply not sensitive enough to detect these waves [13]. Our current detectors, such as ETPathfinder, are tuned to frequencies from 10 Hz to 10,000 Hz in order to detect astrophysical events [14]. Detecting primordial gravitational waves from the Earth is almost an impossible task, as our current methods for detection are based on interferometry, which is extremely sensitive to noise. As can be seen from Figure 1, seismic noise makes it nearly impossible to separate any signal from noise below about 10Hz [15].

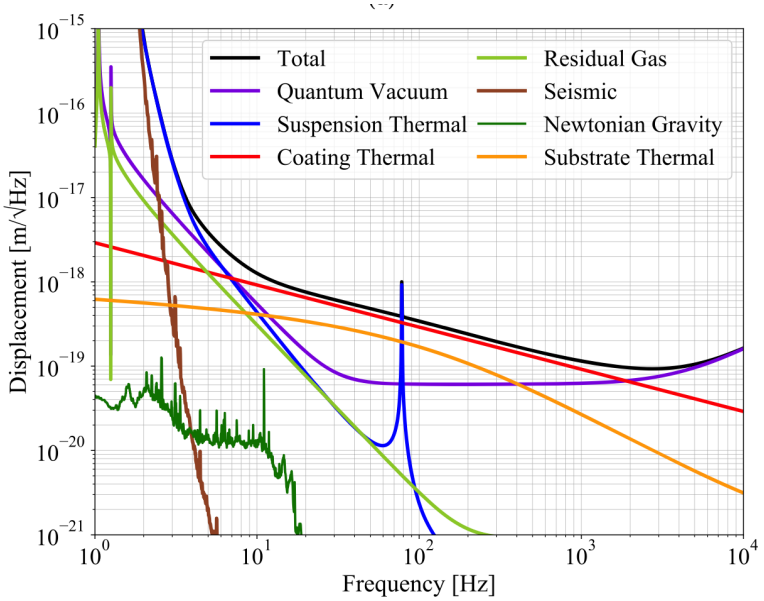

Figure 1: ETpathfinder frequency sensitivty, measurments can only be made above the red line and below the black line.[43]

1.3 Gravitational Wave Detection

The concept of space-based gravitational wave (GW) detectors was first proven in 2015 by the LISA Pathfinder mission [16]. A future space-based GW detector called LISA is planned for launch in 2037 [17]. This detector will be much more sensitive and capable of detecting lower frequency gravitational waves in the range of 0.1 Hz. However, as indicated in Figure 2, this will not be sensitive enough to detect primordial gravitational waves. Nevertheless, its successor, the Big Bang Observer (BBO), may be able to detect some primordial GWs stemming from the electroweak phase transition if certain extensions can be made to the standard model [18]. Currently, detectors cannot be directed like astronomical telescopes and can only roughly estimate the origin of a GW by triangulation.

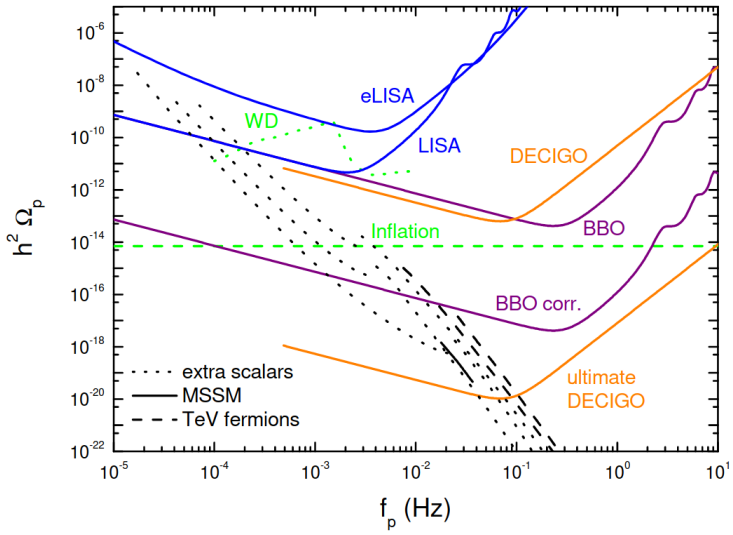

Figure 2: Predicted sensitivity of future reactors, vertical axis depicts the amplitude of the wave, horizontal axis depicts frequency[37].

1.4 Gravitational Lensing as an imaging technique

Gravitational lensing, a phenomenon based on Einstein's theory of the deflection of light in a gravitational field, refers to the bending of light (electromagnetic radiation) or the deformation of space-time (in the case of gravitational waves) due to the presence of massive objects [19]. This bending effect can amplify and distort the images of distant celestial objects, providing a valuable tool for making precise measurements in astrophysics and cosmology [20]. Interestingly, gravitational lensing mirrors the effects of optical lensing, even though it occurs through different mechanisms. Importantly, unlike optical lenses, gravitational lenses affect all kinds of incoming waves, including electromagnetic waves and GWs.

Gravitational lensing could be a useful technique for the detection and analysis of gravitational waves. When a gravitational wave passes through a massive object's gravitational field, the curvature of space-time causes the wave to focus, amplifying the signal [21]. This focusing effect can boost the signal-to-noise ratio, making it easier for detectors to distinguish low-frequency gravitational waves from background noise.

In recent years, researchers have proposed the use of the Sun as an optical lens to study exoplanets within our stellar neighborhood, as using classical methods such as telescopes and interferometers requires very precise measurements and an unfeasible amount of time [43]. We know that the Sun has a gravitational focal length for optical light of around 550 AU [36], and if we were able to place a probe at this distance it would be able to take measurements of

exoplanets with unprecedented resolution, giving us information on topography, climate, and geography of these exoplanets [43].

1.5 Our Design for a Space-Based GW Detector

The limitations of current gravitational wave detectors primarily center around their inability to be directed. Given the universal and constant nature of gravitational waves, they arrive from all directions, which poses significant challenges for traditional detection methodologies. We propose a paradigm shift in our approach to detecting these elusive waves. Instead of using conventional, non-directional detectors, we suggest the use of a satellite-based gravitational wave detector that can be aimed.

The idea is to leverage the Sun's gravity as a natural and powerful lens for amplifying the gravitational wave signals. This concept is akin to using a magnifying glass to concentrate light. By placing our satellite detector in an orbit around the Sun, we create the possibility of scanning the sky directly behind the Sun. As the satellite orbits, it can continuously adjust its direction to focus on different points behind the Sun, allowing for a comprehensive scan of the celestial sphere.

Another important aspect of our proposed system is its capability to detect a constant source of noise, rather than looking for individual, isolated events. Gravitational wave detectors typically search for short-lived, high amplitude signals caused by violent cosmic events such as the merger of black holes or neutron stars. However, our system aims to detect the continuous, "humming" background noise of gravitational waves. These waves are thought to be produced by a myriad of less dramatic, but far more frequent, cosmic events, as well as potentially by phenomena from the early universe.

By focusing on this gravitational wave background noise, we can potentially gain new insights into the broader dynamics of the universe. Furthermore, the proposed design enables a consistent and systematic method for gathering and interpreting gravitational wave data. Instead of waiting for rare and unpredictable events, this design allows for a continuous collection of data, thereby opening new possibilities for astronomical discovery and understanding.

This new design could potentially revolutionize the way we detect and interpret gravitational waves. However, it also brings its own set of challenges and technical hurdles that will require innovative solutions. Among these are maintaining stable communication with a distant probe and mitigating the effects of solar electromagnetic radiation, both of which are currently being addressed in the field of gravitational wave astronomy [13, 17].

Addressing the directional limitations, we propose the idea of employing a satellite gravitational wave detector that can be aimed to scan the celestial sphere. By using the Sun to amplify incoming signals, we propose launching a satellite or a swarm of satellites in a precessing elliptical circumpolar orbit around the Sun, similar to the orbit followed by Mercury which can be seen in Figure 3.This allows the satellite to take images at different distances. This maneuver will use the Sun as a gravitational lens to amplify oncoming signals.

This approach could potentially enable space-based detectors, such as LISA, to detect primordial gravitational waves, an achievement it may not otherwise be able to accomplish. The initial design plan involved positioning the apparatus at the Sun's focal length, but at 550 AU, the orbital period would be 12,897 years. A full picture of the sky would require the satellite to make multiple orbits around the Sun. Therefore, the location must be carefully selected to maintain a reasonable distance from the Sun for accurate readings, without becoming infeasible due to time constraints. A trade-off must be made between imaging power and orbital period. To overcome this constraint, we propose sending a swarm of satellites, each starting at a different position above the Sun, enabling simultaneous readings of different parts of the sky, thereby limiting the number of orbits necessary for a full image. A gravitational wave detector similar to LISA would be aboard this hypothetical satellite [16].

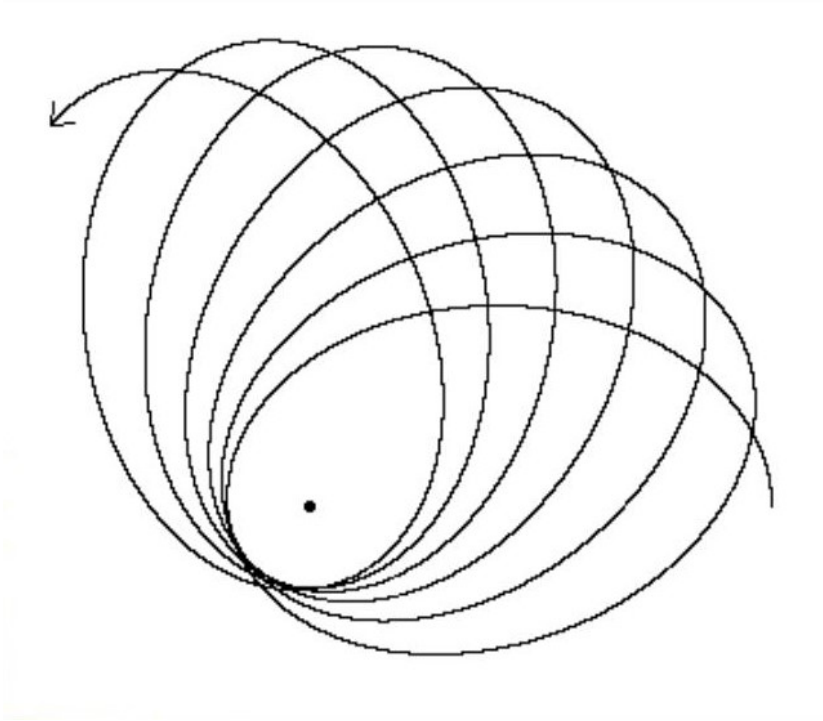

Figure 3: Mercury's precessing orbit.[52]

1.6 Technical Challenges

Gravitational waves interact weakly with matter, making their direct detection extremely difficult; unlike EM waves, they also pass directly through the Sun [21]. Lensed gravitational waves would also have to be distinguished from local sources of gravitational waves and other potential noise sources, which may require the development of advanced data analysis techniques to accurately identify and characterize lensed gravitational wave signals [7].

One way to overcome some of the above-listed limitations would be to make a simplified model of the Sun and calculate the path a gravitational wave would take as it passes through its gravitational field. By calculating the path of GW coming from infinity and their deflection in the Sun's gravitational field, we aim to predict how the Sun would lens the GW skymap and ultimately reveal the lensed image. It is worth noting that lensing has been observed for many years in astronomy, however, GW lensing by black holes is mostly (99%) observed near the event horizon [24]. This yields an effect that is much more prominent than lensing by the Sun, which is due to the strength of the effect of lensing by a black hole, meaning the effect is much less concentrated and hence weaker [25].

As mentioned earlier, gravitational lensing causes large distortions to appear in images when not observed from the focal length, much like regular optical lenses. Due to this effect, any realistic measurement that we can make using the Sun as a gravitational lens, would be affected by this distortion. This effect must be compensated for somehow. When it comes to optical lenses, distortions within the lens are fixed by adding a secondary lens which corrects the image, called a *collimator*. This is an appropriate solution for optical lensing. However, in the case of gravitational waves lensed by the Sun, it would not be as simple as placing another detector to correct the error. The correction must be done in some other way. For this, we propose the use of AI as a software collimator. Machine learning, a sub-field of artificial intelligence (AI), has already been used in several other studies showing its ability to correct images in astronomical telescopes and space telescopes [26]. Deep learning, a sub-field of AI , focuses on emulating the learning approach that humans employ to acquire specific types of knowledge [49]. Characterized by the application of neural networks with several layers, these 'deep' structures aim to mimic the neural network of the human brain, thus the term 'deep learning' [50]. The pioneer in this field, Geoffrey Hinton, has significantly contributed to the evolution of deep learning algorithms, fostering their use in a myriad of domains from image recognition to natural language processing, and potentially in gravitational wave lensing [51].

This thesis will explore the underlying mechanism of gravitational lensing for gravitational waves, building on the growing body of literature on this topic. It aims to investigate the feasibility of using the Sun as a gravitational lens, delving into the underlying principles, technical challenges, and potential applications for both gravitational wave detection and correction of lensing distortions. The focus of our work will be on the designing of an AI-based collimator [27].

2 Theory

2.1 Deflection of Gravitational waves by the Sun

The path of gravitational waves that are deflected by the Sun can be distinguished in two types: (i) passing past the Sun, (ii) passing through the Sun. These paths are described by general relativity, for a good introduction see the book "Graviatation"[44] The first type is determined entirely the Schwartzschild metric, the second is more complicated and is determined by the distribution of mass and pressure inside the Sun. We briefly describe the methodology necessary to find these two types of paths. In both cases, the paths are geodesic solutions subject to the appropriate metric tensor $g_{\mu\nu}$:

$$\frac{du^\alpha}{d\lambda} = \Gamma^\alpha_{\mu\nu} u^\mu u^\nu \tag{1}$$

The non-tensorial Christoffel affine connections $\Gamma^\alpha_{\mu\nu}$ are directly derived from the metric tensor in the following way:$g_{\mu\nu}$.

$$\Gamma^\alpha_{\mu\nu} = \frac{1}{2} g^{\alpha\lambda} \left(\frac{\partial g_{\lambda\mu}}{\partial x^\nu} + \frac{\partial g_{\lambda\nu}}{\partial x^\mu} - \frac{\partial g_{\mu\nu}}{\partial x^\lambda}\right) \tag{2}$$

Solving this differential equation with the appropriate boundary condition, we can obtain the deflection angle θ as z approaches $+\infty$.

It's important to note that the specific form of $\rho(r)$ and $P(r)$ will determine the exact expressions for the Christoffel symbols and the subsequent solution for θ. These equations provide a general framework to follow in solving for the deflection angle in the scenario described.

2.1.1 Geodesic paths outside the Sun

For the first case, outside the Sun, the solution is well-known, namely the Schwartzschild metric:

$$ds^2 = -\left(1 - \frac{r_s}{r}\right) dt^2 + \left(1 - \frac{r_s}{r}\right)^{-1} dr^2 + r^2 d\Omega^2 \tag{3}$$

where $r_s = \frac{2GM}{c^2}$ is the Schwarzschild radius, G is the gravitational constant, M is the mass of the central object, c is the speed of light, t is the time coordinate, r is the radial coordinate, and $d\Omega^2 = d\theta^2 + \sin^2\theta d\phi^2$ is the line element for the unit 2-sphere. Moreover, the deflection of a horizontal in-falling GW ray with impact parameter $d > R$ due to a spherical symmetric mass M can be given by the following equation predicted by Einstein in 1919 and confirmed by Dyson and Eddington 1 year later [45]:

$$\delta\theta \approx \frac{4GM}{c^2 d} \tag{4}$$

where $\delta\theta$ is the deflection angle, G is the gravitational constant, c is the speed of light, and d is the closest distance of approach of the light ray to the center of mass M.

2.1.2 Geodesic paths through the Sun

The second scenario, the GW ray passing through the Sun, is more intricate, as we first have to find the Christoffel symbols inside the Sun, based on a physical model of its mass-energy distribution [1].

We model the Sun as an ideal fluid with a spherical symmetric mass density and pressure distribution, given by $\rho(r)$ and $P(r)$ respectively. These in turn, we assume, are modelled by *simple stellar models*, a set of differential equations for stellar structure and evolution. Notably, for the Sun, these are the equilibrium structure equations of stellar models for the Main Sequence.

$$\begin{aligned} \frac{dP}{dr} &= -\frac{Gm(r)\rho(r)}{r^2} \\ \frac{dm}{dr} &= -4\pi\rho(r)r^2 \end{aligned} \tag{5}$$

The functions $\rho(r)$ and $P(r)$ for a stellar model depend on the specific assumptions made about the equation of state and energy transport mechanisms, as well as the boundary conditions at the surface and the center of the star For our simple model we use the solution provided by Kippenhahn and Weigert [47], depicted in Figure 3

In order to compute the Christoffel symbols and geodesics,we first need to solve the Einstein Field Equations (EFEs) for a spherically symmetric energy-momentum tensor $T_{\mu\nu}$ containing the mass density $\rho(r)$ and pressure $P(r)$.
The energy-momentum tensor for a spherically symmetric mass distribution can be written as:

$$T_{\mu\nu} = \begin{pmatrix} \rho(r)c^2 & 0 & 0 & 0 \\ 0 & P_r(r) & 0 & 0 \\ 0 & 0 & P_\theta(r) & 0 \\ 0 & 0 & 0 & P_\phi(r) \end{pmatrix} \tag{6}$$

where $\rho(r)$ is the spherically symmetric mass density, $P_r(r)$ is the radial pressure, $P_\theta(r)$ is the pressure in the θ direction, and $P_\phi(r)$ is the pressure in the ϕ direction. We now insert the results from Eq 5, and use that the pressure is spherically symmetric and purely radial; so $P_r(r)$ is given by the solutions $\rho(r)$ and $P(r)$ from Eq 5, and the tangential pressure and azimuthal pressure vanish: $P_\theta = 0$, and $P_\phi = 0$. This leads to $T_{\mu\nu} = \text{diag}(\rho(r)c^2, P(r), 0, 0)$.

The next step to obtain the geodesic equation is to solve the EFEs for this energy-momentum tensor $T_{\mu\nu}$. In order to do so, we parameterize the metric tensor as:

$$ds^2 = -e^{2\Phi(r)}dt^2 + e^{2\Omega(r)}dr^2 + r^2(d\theta^2 + \sin^2\theta d\phi^2) \tag{7}$$

[1] A common reference for the equations of stellar structure is the book "An Introduction to the Theory of Stellar Structure and Evolution" by Dina Prialnik, which provides a comprehensive treatment of the subject. Other standard references include "Principles of Stellar Evolution and Nucleosynthesis" by Clayton, "Stellar Structure and Evolution" by Kippenhahn and Weigert, and "Introduction to Stellar Astrophysics" by LeBlanc and Wilson.

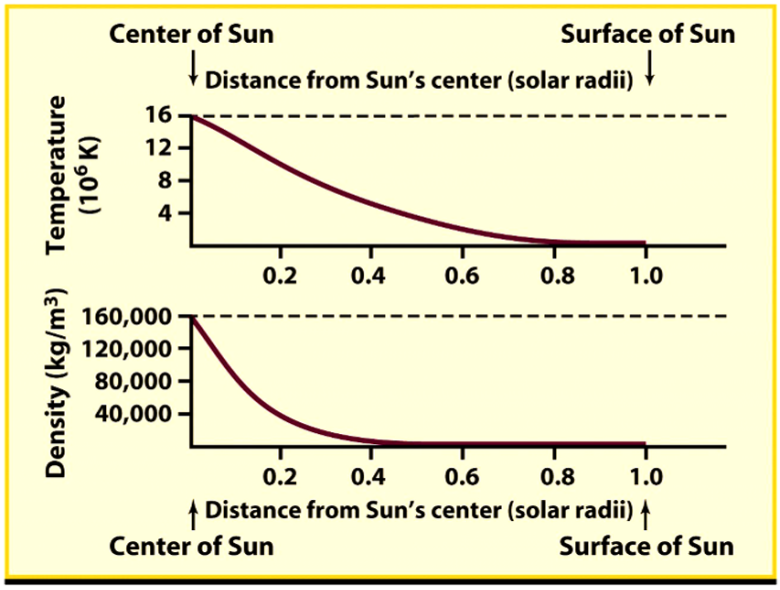

Figure 4: Standard Solar Model. From: The Astronomy Department at the California Institute of Technology

which represents the metric on the unit 2-sphere, and $\Phi(r)$ and $\Omega(r)$ are functions of the radial coordinate r only.

The EFEs for this energy-momentum tensor are:

$$R_{\mu\nu} - \frac{1}{2}g_{\mu\nu}R = \frac{8\pi G}{c^4}T_{\mu\nu} \tag{8}$$

where $R_{\mu\nu}$ is the Ricci tensor, R is the scalar curvature, $g_{\mu\nu}$ is the metric tensor, and $T_{\mu\nu}$ is the energy-momentum tensor.

The EFEs for this metric and energy-momentum tensor reduce to two coupled second-order ordinary differential equations for $\Phi(r)$ and $\Omega(r)$. These equations are known as the Tolman-Oppenheimer-Volkoff (TOV) equations[48][2].

,

The TOV equations for a spherically symmetric system with mass density $\rho(r)$ and radial pressure $P(r)$ are

$$\begin{aligned} \frac{d\Phi}{dr} &= -\frac{Gm(r)}{r^2}\frac{(\rho(r)+P(r))}{1-\frac{2Gm(r)}{rc^2}} \\ \frac{d\Omega}{dr} &= 4\pi r^2\frac{(\rho(r)+P(r))}{c^2} \end{aligned} \tag{9}$$

[2]for a detailed discussion see "Gravitation"

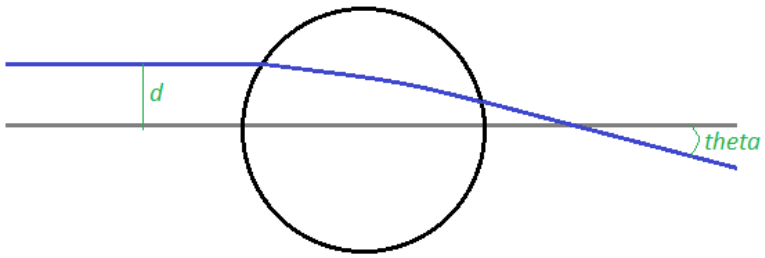

Figure 5: Rough Sketch Geodesic Solar Deflection, showing a Gravitational wave entering the Sun at impact parameter d resulting in a deflection angle θ.

where $m(r)$ is the total mass enclosed within radius r, and follows from: $\frac{dm}{dr} = 4\pi r^2 \rho(r)$. The functions $\Phi(r)$ is the gravitational potential, and $\Omega(r)$ are the gravitational potential and space time curvature respectively. The first equation gives the gradient of the gravitational potential, the second relates the curvature to the matter distribution.

Once we have numerically solved for $\Phi(r)$ and $\Omega(r)$ for the given solar density $\rho(r)$ and pressure $P(r)$, we can compute the Christoffel symbols $\Gamma^{\alpha}_{\mu\nu}$ and use them to compute geodesics in the space-time from Eq 1 .

2.2 Computation of the deflection from the Geodesics

Once we have obtained the Christoffel symbols $\Gamma^{\alpha}_{\mu\nu}$, we can numerically solve the geodesic equation Eq 1 with the correct boundary conditions. The boundary conditions concern an incoming GW ray parallel to the axis at $-\infty$ and directed at an angle θ at $+\infty$.

We take spherical symmetric coordinates (r, ϕ, θ) and take the z-axis as main axis. The centre of the Sun is located at the origin. Let R be the radius of the Sun. In the region I: $r > R$ we assume the Schwartzschild metric $g^{S}_{\mu\nu}$. In the region II: $r \leq R$ we assume the TOV-metric $g^{TOV}_{\mu\nu}$. Note that even in region I the geodesics are curved, hence a ray parallel to the z-axis at distance d at $z = -\infty$ will hit the Sun at a somewhat smaller distance d' to the z-axis. This small effect, however, we will ignore in our simple model.
As boundary conditions we assume a GW ray at a distance d parallel to the z-axis and take: $u^r(-\infty) = 1$, $u^{\theta}(-\infty) = 0$, and $u^{\phi}(-\infty) = 0$.
Next, we solve the geodesic equation Eq 1 in the appropriate regions I and II, and study the solution $u^{\mu}(\lambda)$ for $\lambda \to +\infty$. The deflection angle θ follows from: $\tan\theta = u^{\theta}(\infty)/u^{r}(\infty)$. Fig. 5 shows the relation between deflection angle θ and the impact parameter d.

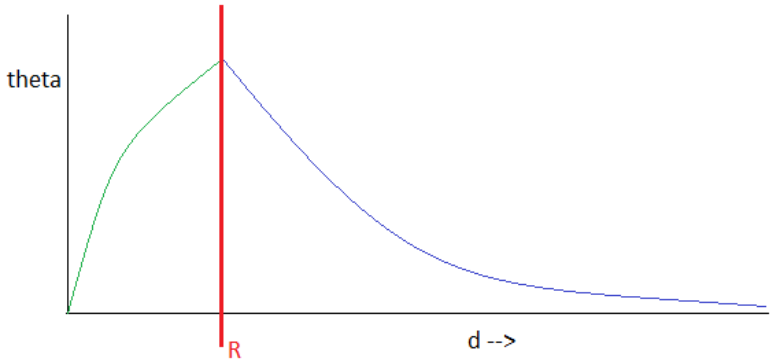

Figure 6: Graph of deflection angle θ versus the impact parameter d.

3 Methods

3.1 Simplified Model for Lensing

Here we introduce a simplified and practical approximation of the theory presented in Section 2. Our starting point was conventional geometric optical lensing as a solution. Since, as stated earlier, the phenomenon of gravitational lensing and optical lensing give very similar outcomes, we decided to use an approach which treats the lensing effect by the Sun as a pixel transformation. We did this by first defining an optical axis and placing an imaginary point at infinity from the Sun. We needed to define two parameters which are the impact parameter – the distance the object is from the optical axis – and the distance of the observer to the Sun see fig. 4. These were named b and a respectively. We then defined the deflection angle as θ. By doing this we were able to use geometric approximations and find that the new x and y coordinates after the transformation would be equal to: $(x_p, y_p) = d(x, y\,)r/b\,\tan(\theta) - (x, y)$. Below in Figure 7 from Turyshevs paper [40], from which inspiration was taken. We used this approach, however we simplified the rays to have straight paths so that we were able to form triangles which we could use to predict the deflection angle.

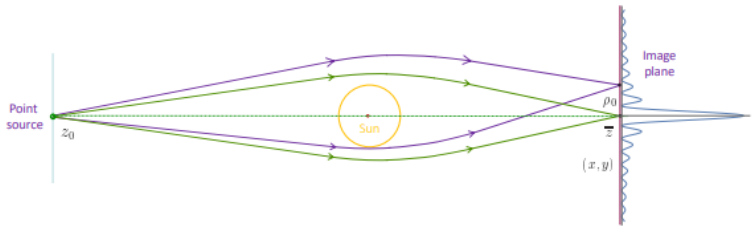

Figure 7: Image taken from turyshevs paper, demonstrating rays from a point source passing the Sun and being lensed[40]

As was discussed in the theory Section, we must distinguish between the two types of paths waves can taken. For the gravitational wave passing past the Sun we were able to use Schwarzschild metric and results from Clifford Will [46] we were able to find the formula to describe the transformation that would happen to the gravitational wave under Schwarzschild metric. Through the Sun the task becomes significantly more complex as described in the earlier Sections. However, according to Figure 6 and due to the almost insignificant nature of the effect of gravitational lensing by the Sun we have decided to simply use a linear relation for waves passing through the Sun as we expect this should be almost identical to real effect which will not be very pronounced.

3.2 Generation of Test Data

Our first attempt at generating images of the Sun's lensing effect were initially done through the use of the Python library *Lenstronomy*, a library dedicated to the simulation of gravitational lensing [41]. Unfortunately, Lenstronomy has several limitations when it comes to this type of simulation. Lenstronomy is designed to simulate large mass lensing, for example from galaxies and supermassive black holes, and it is very good at this task, however it was not designed for smaller objects. Lenstronomy comes with several equations of state for simulation, but none of them describe a stellar object. This meant we had to simulate using the Sun as a point mass (effectively a black hole), which meant that we were not able to simulate the lensing effect of the Sun with Lenstronomy, though we are able to simulate the lensing effect of a black hole with the Sun's mass.

Using the approximation as explained in Section 3.1, a data set containing 44 characters, including the whole alphabet numbers, and some additional symbols was generated and then put through Python code which was able to use the results obtained under the approximation in Section 3.1 to generate images under different values of r, starting at 0.25 AU and going up to 4 AU. The code would recreate the images as lensed by the Sun according to our approximation. These images were generated for two purposes, firstly as a proof of concept for us to understand how the images would appear lensed by the Sun at different distances and secondly to be later used to train a machine learning algorithm

which would be able to look at the distorted images and reconstruct to the original.

3.3 The Concept of Using an AI Collimator

We chose to use letters as they are highly structured images which would make it clear what effect the Sun's lensing has on gravitational waves. In order for machine learning algorithms to produce reliable results clear patterns must be present in the images. Both are the reasons why we did not use something like the CMB or stochastic noise as both of these are prone to randomness. In order to prepare the images for machine learning they first to be one hot encoded. This being the process of taking the features from the image and putting them in an array of zeros and ones where the position of one in the array correspond of the feature of the image. The data was split into training and testing using an 80 – 20 split and some data augmentation was used on the images in order for the algorithm to be more generally applicable as it forces the algorithm to learn more patterns and prevent over-fitting. The reason for using different distances from the Sun was to have sufficient data as well as to achieve better generalization of the machine learning algorithm. Having 44 characters recorded at six different distances from the Sun would be an excellent data set for a machine learning algorithm as they would be patterns easily recognizable and easy to a human observer to confirm. The machine learning algorithm was trained to recognize the features of the image. Once the algorithm was trained confusion matrix was generated to see if there were any issues with particular characters or if it would frequently get confused by two similar looking characters. True reconstruction of the image was not made, instead in order to test the algorithm it was shown a letter at the distance it had never seen and asked to label it and redraw it from the original image. With these methods we are able to get an approximation of how gravitational waves would appear if lensed by the Sun at sub-focal distances like 1 AU and have a proof-of-concept method of reconstructing the image.

4 Results

4.1 Effects of lensing by the Sun at sub-focal distances

As discussed earlier, letters and characters were chosen to be used for a simulation of Sun's lensing effect. Some selected letters are presented in Figures 9a, 9b and Figures 10a, 10b and they demonstrate the Sun's lensing effect. The examples below are selected as they do not have any geometric symmetry, which better demonstrates the mirroring effect of the lensing and also demonstrates clearly how the impact parameter influences the distortion. We also present an example image, showing the center of the optical axis and an outline of the Sun, which can be found in Figure 8.

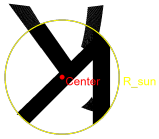

Figure 8: Distortion of the letter K with our simplified approx, showing the Sun and optical axis center

(a) Predicted distortion using our approx. for the letter M at 4 AU

(b) Predicted deflection using our approx. for the letter M at .25 AU

Figure 9: Predicted distortion using our approx. for M at separate distances

(a) Predicted deflection using our approx. for the letter K at 4 AU

(b) Predicted deflection for the letter K at 0.25 AU

Figure 10: Predicted distortion for K at separate distances

Figures 11a and 11b presented some results form our initial round of simulations which used lenstronomy which approximated the Sun as a Black Hole. However, the results are ultimately not useful due to the fact that for a black hole a majority of lens effect occurs near the event horizon. For an object with the mass of the Sun its event horizon is only 3 km which is not a very large area meaning that we do not observe any lensing effects for objects placed very far away from the optical axis.

(a) Predicted deflection for the letter B at 1 AU using lenstronomy

(b) Predicted deflection for the letter B at 138 AU using lenstronomy

Figure 11: Predicted deflection for 2 separate letters

4.2 Predicted deflection angle

In Figures 13 we show a prediction for the Sun's lensing effect, specifically how the deflection angle will change with the impact parameter. Below is an image which shows the outcome from the simulation excluding impact parameters from within the Sun. As stated earlier we predict this to be a relationship between deflection angle and impact parameter smaller than the radius of the Sun to be almost linear. Also due to the weakness of the effect even if it is not linear, the resulting amplitude of this effect is likely going to be very small, making it so that we are comfortable with our approximation.

The deflection angle was first calculated for each letter individually, as can be seen the predictions appear quite similar, which is promising. We expect this effect of the Sun's lensing to be consistent for each letter, as they were all made the same font size, therefore should have almost the exact same deflections occurring.

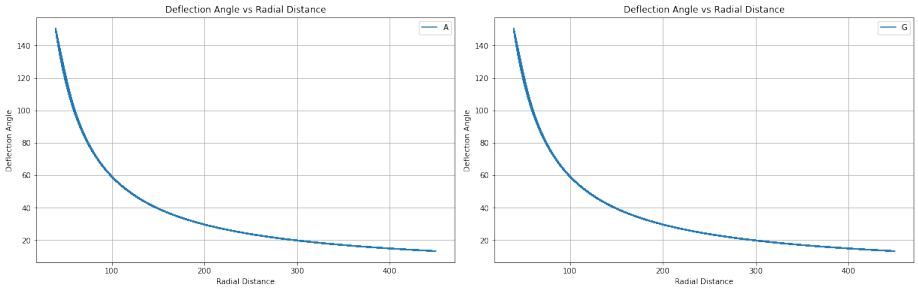

(a) Predicted deflection for the letter A (b) Predicted deflection for the letter G

Figure 12: Predicted deflection for 2 separate letters

To make a final estimation, all the values for each letter were averaged out, and an aggregate plot was made, predicting the half of the graph shown in figure 3, and confirming that our approximation was effectively implemented.

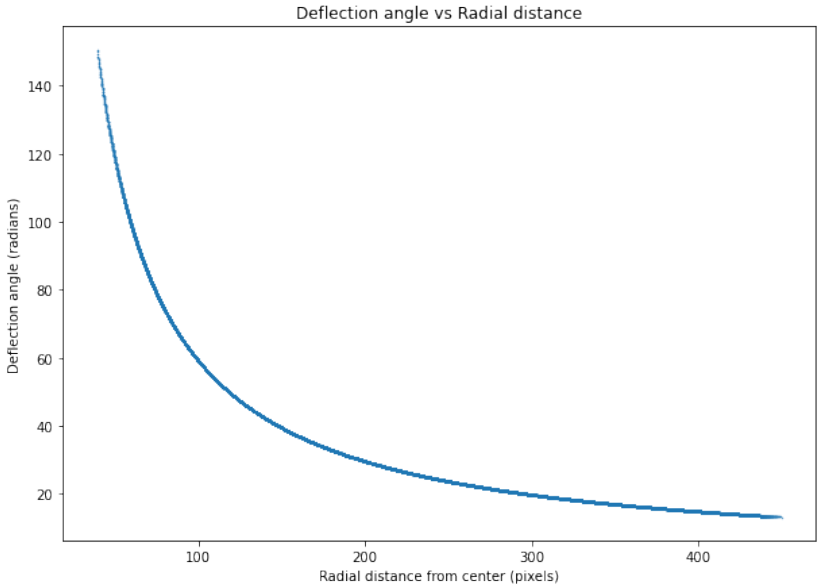

Figure 13: Our predicted (average) values for the deflection angle plotted against radial distance from the optical axis

4.3 Reconstruction of distorted lensed images

As stated in the Methods Section machine learning algorithm was trained on the results of the simulation of the Sun's lensing effects on the letters. Below we display a confusion matrix which displays how prone the algorithm is to mistakes

as well as if there are any letters or symbols in specific which it seems to have troubles with. Below two examples are shown of the algorithm predicting the original image from its distorted counterpart, the letter B is shown at 1 Au, and the letter Y at .5 AU, demonstrating that our AI is capable of understanding out what was in the original.

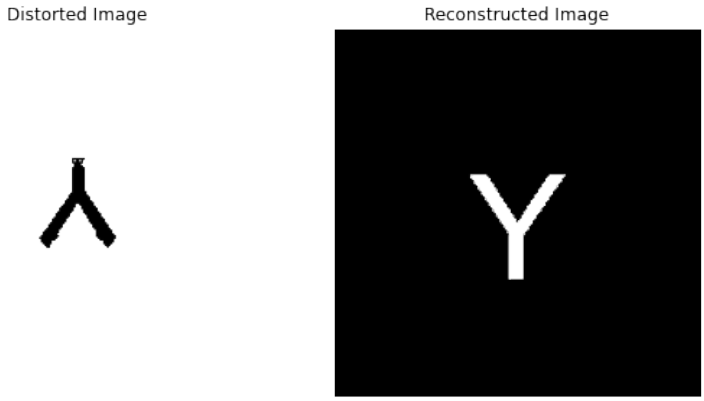

Figure 14: AI being shown an image of a Y at 0.5 AU and guessing the original

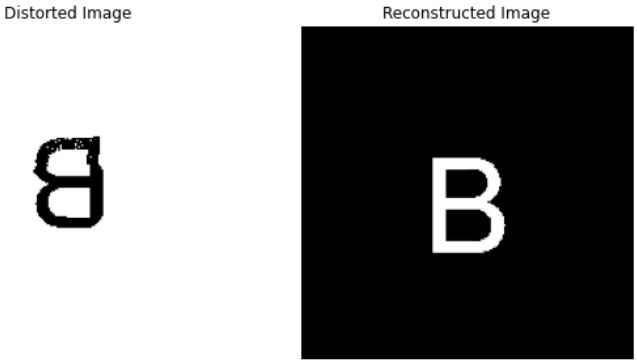

Figure 15: AI being shown an image of B at 1 AU and guessing the original

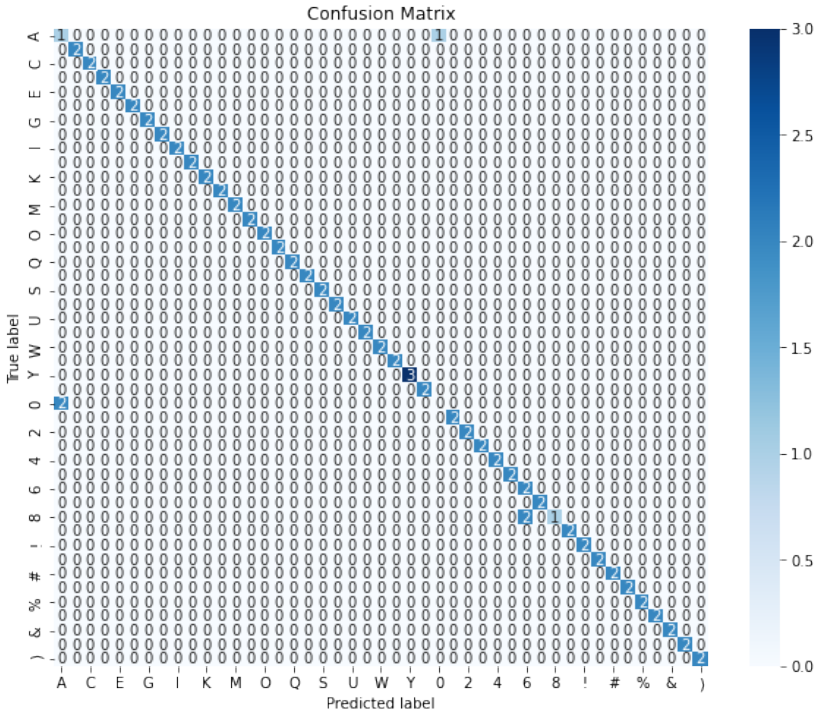

Figure 16: Confusion matrix for our AI, axes are folded due to number of features.

	precision	recall	f1-score	support
A	0.33	0.50	0.40	2
B	1.00	1.00	1.00	2
C	1.00	1.00	1.00	2
D	1.00	1.00	1.00	2
E	1.00	1.00	1.00	2
F	1.00	1.00	1.00	2
G	1.00	1.00	1.00	2
H	1.00	1.00	1.00	2
I	1.00	1.00	1.00	2
J	1.00	1.00	1.00	2
K	1.00	1.00	1.00	2
L	1.00	1.00	1.00	2
M	1.00	1.00	1.00	2
N	1.00	1.00	1.00	2
O	1.00	1.00	1.00	2
P	1.00	1.00	1.00	2
Q	1.00	1.00	1.00	2
R	1.00	1.00	1.00	2
S	1.00	1.00	1.00	2
T	1.00	1.00	1.00	2
U	1.00	1.00	1.00	2
V	1.00	1.00	1.00	2
W	1.00	1.00	1.00	2
X	1.00	1.00	1.00	2
Y	1.00	1.00	1.00	3
Z	1.00	1.00	1.00	2
0	0.00	0.00	0.00	2
1	1.00	1.00	1.00	2
2	1.00	1.00	1.00	2
3	1.00	1.00	1.00	2
4	1.00	1.00	1.00	2
5	1.00	1.00	1.00	2
6	0.50	1.00	0.67	2
7	1.00	1.00	1.00	2
8	1.00	0.33	0.50	3
9	1.00	1.00	1.00	2
!	1.00	1.00	1.00	2
@	1.00	1.00	1.00	2
#	1.00	1.00	1.00	2
$	1.00	1.00	1.00	2
%	1.00	1.00	1.00	2
^	1.00	1.00	1.00	2
&	1.00	1.00	1.00	2
(	1.00	1.00	1.00	2
)	1.00	1.00	1.00	2
accuracy			0.95	92
macro avg	0.95	0.95	0.95	92
weighted avg	0.95	0.95	0.94	92

Figure 17: Statistical tests for our AI, showing error

In Figure 17 we present some statistics for our AI and a confusion matrix in Figure 16. we can see that the AI makes good predictions, correctly guessing most letters, apart from A, which it often confuses with a 0, and 8, which is confused with a 6. These results make sense, as the 'Squishing' effect of the lensing make some images almost indistinguishable. We also present the results of some statistical tests, confirming where our algorithm makes mistakes. Overall however, achieving an accuracy of 95% on its testing data is extremely impressive. The algorithm is also able to handle new images it is shown, for example the B and the Y shown in Figures 15 and 14 . As long as we present it with a distorted letter it has seen it should be able to make an accurate prediction. Care must be taken when showing images similar to the ones which it is known to make mistakes on.

5 Discussion and conclusion

The results give us an overview of how we predict the Sun's lensing effect would appear for different objects at different distances from the Sun. We also demonstrate a prediction for how the deflection angle changes with the impact parameter at least for impact parameters larger than the Sun. Also a proof of concept machine learning algorithm is provided which is able to learn how the Sun's lensing effect affects letters and symbols and is able to reconstruct the original image.

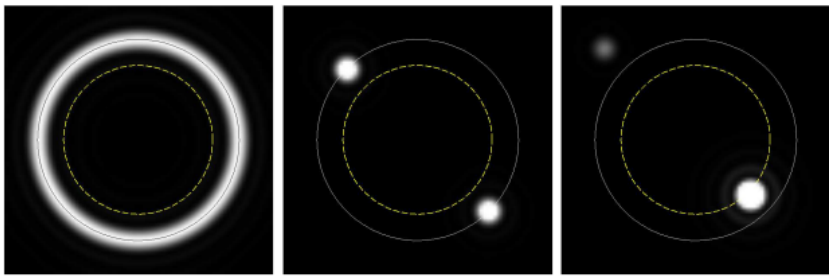

Figure 18: Turyshev's simulataion of images 1000 AU from the Sun on different axis[40]

Comparing our lensing simulation to the results from Turyshev's 2020 paper in Figure 18 [40], we do not observe the exact same lensing effects he predicts. However, three things are of importance to note: (i) in comparison to Turyshev's paper, as stated in Section 3.1, a more simple approach was used, (ii) the simulation by Turyshev does not use any structured objects to show the lensing effect; our research uses the letters and symbols and as highly structured images they cause a significantly less pronounced Einstein ring, and (iii) the paper tests extreme distances of a 1000 AU which are not useful for any practical purpose and also the larger distance from the focal length will cause a more significant

distortion, further the images on the right and center are taken off axis, so we will not compare to them.

5.1 Cost and Operation of a Hypothetical Directed GW Detector

One must consider the feasibility of sending a satellite to orbit the Sun and use it to measure gravitational waves. This is highly hypothetical and simplified estimation of the feasibility and cost of such an operation. This discussion will partially be based on information of expected cost of public information available on other satellites and the gravitational wave detectors [28]. We should bear in mind detailed cost breakdowns and expenses for these missions are typically not given or given in a short-summarized form without many details [29]. One of very important characteristics is the weight of the satellite. As cost of LISA mission is not publicly disclosed, we will estimate costs based on cost of the Mars Science Laboratory Mission that carried Curiosity vehicle to Mars, which was reported to cost around 2.5 billion USD and weighed 899 kg [30]. LISA is estimated to weigh 6.9 tons, having three parts weighing 2.3 tons each [17], so we can assume that our satellite would be somewhere in this approximation.

We will split the cost into several categories and try to use as accurate information as possible. The cost can be split into six categories: (1) development and construction (2) launch (3) communication (4) operation and data analyses (5) fuel and maintenance and (6) end of life planning. For the Mars Science Laboratory mission 1.5 billion USD out of 2.5 billion USD was spent on development and construction. This being 60% of the budget seems like a reasonable estimate for our case although depending on how much innovation it is required for our project this could be a higher percentage. For the launch of the Curiosity they used the Atlas V rocket and it cost in the range of $120 - 200$ million USD. This rocket is capable of carrying our satellite as long as we launch each part of the satellite individually, therefore this can be taken as the cost of launching our satellite multiple by three. For the Curiosity mission the communication was estimated to cost tens of millions USD and for our case communication is more complex and delicate and therefore the cost increase is inevitable being somewhere in the order of one hundred million USD. Operation and data analyses follow the same pattern as described for communications and thus we estimate it to be in the same range. Fuel and maintenance can not be estimated at this moment as we are unsure how long the mission would last and similarly applies for end-of-life planning.

LISA is estimated to cost several billion euros [31] and we estimate that our satellite would be in this range or even more expensive due to necessity to develop the new technologies to handle the Sun's lensing effect. Most of the funding would be utilized for the first two categories with others being incalculable for us at the moment.

We can make some estimates about how long it will take to get the full GW skymap, but first some assumptions must be made about our measurements. Assume our satellite is able to scan about 20 degrees every time it goes around

the Sun, to get a full GW skymap, we must then make 18 orbits around the Sun, or, if we place the satellite at 1 AU, about 18 years [33]. This is of course under the assumption that after one single full scan of the sky, we will get a perfect image of the GW skymap, however this is unlikely. It will probably take us more measurements to get a good image, maybe 10 or more full rotations, or 180 orbits. This seems too long for any experiment, and would also hugely increase costs, as this is effectively 180 years of fuel, people to read data, and many other expenses. This means we must place the satellite closer to the Sun and reduce its orbital period. By placing it at .25 AU, we reduce the orbital period to 1/10th of a year, meaning 180 orbits can be done in 18 years. Of course the image quality will be worse, so we can do for example 400 orbits over 40 years to make up for the increased lensing effect of the Sun at this distance. As can be seen in the Results Section, at 0.25 AU, the lensing becomes very strong and unfocused, strongly distorting the image seen. This is why an AI collimator is necessary to this project, as to make reasonable measurements without some sort of correction is impossible in the foreseeable future.

5.2 Challenges and advantages of our methodology

We are confident in the approximations that we have made in this study and that the constraints of the approximations have not had a significant bearing on the value of the results. A choice that was made for the purposes of simplicity and demonstration of this as a proof of concept was to ignore the scattering effect of gravitational waves and EM radiation, at a single point they are not emitted in one direction but rather in a full sphere around the point. This would mean that a single point on a single source would in reality lead to multiple points observed in a lensed image. We expect that this effect would add to distortion present in the lensed images. Even if a future implementation were including the scattering effect, our method of gravitational imaging from Section 3.1 would still be perfectly applicable to the example as they are able to simulate the path of the gravitational wave being lensed by the Sun, although these results would appear significantly more distorted than ours. It is also important to note, gravitational lensing is *deterministic*, and so is our algorithm. For the same input the same output will always be given.

For a proof of concept of training the machine learning algorithm to be able to reverse the lensing effect of the Sun our obtained images are still perfectly usable and serve as a good baseline for future research.

One other limitation, with machine learning in general, and not just with this research, is that it is extremely difficult for it to make predictions on completely new patterns meaning that finding a data set for this hypothetical AI collimator for a gravitational wave detector would prove to be a difficult task as we do not have any example of how a primordial gravitational wave would appear at all, lensed on not lensed by the Sun.

This research serves as a good basis for future research in the field of detecting the gravitational wave background as well as using the Sun to make cosmological and astrophysical observations. We also hope that the idea of an

AI collimator will be explored further in this field as there may be ways around the limitations discussed above. Already AI collimators are being used in other areas of cosmology by being used to help researchers detect objects in space. We also hope that our simulations and methods, while simple, could potentially be improved upon by future researchers or even used as proof of concept for new technologies in this field.

The most obvious immediate improvement that can be made on our research is the accuracy of the lensing simulation. As discussed in Section 3.1 and in this Section, there were some limitations and simplifications in our methods. For example, one thing that could be done would be to apply the theory discussed earlier in order to accurately find the deflection angle for gravitational waves passing through the Sun. While waves which pass beyond the Sun are easily described and can be simulated with Schwarzschild metric there are suitable simplified models within the Sun such the TOV offers a suitable approximation that can be used.

Despite the recent discovery made by the NANOgrav group [53], we still argue that this research is important, for two reasons of note. Firstly, and most simply, the group has not proposed how they will measure the skymap, and it is unclear if their method will yield the skymap at all, however, using our method, we are directly measuring the skymap, there is no question whether or not our research will find it if it were to be carried out, as it is what we are directly measuring. Secondly, even if the method put forth by the NANOGgrav group is superior, it is still good science to have two separate measurements of the same phenomenon, as it allows for comparison and accelerates scientific growth. Further, it is important to note their methods have some benefits compared to the ones laid out in this paper, the most important one being the cost is significantly cut down. However, this paper also gives hopeful progress, as it corroborates the existence of primordial waves, which make this experiment much more feasible to carry out in the future.

5.3 Conclusion

If the results of this research lead to the detection of primordial gravitational waves it would strongly improve our understanding of the universe, its formation, inflation, early events which we are currently unable to describe or observe. As with any other rapid advancement in any scientific field alongside come new technologies which could permanently change human civilization. At this stage we can not hope to even launch a small scale test satellite as least not until the development of LISA is completed. As our research was mostly exploratory in nature and due to its novelty, we did not go in with any particular expectations for how our results will appear. However, we can conclude that they are in line with what we would expect to observe.

Assuming all the steps would be followed, the end result of this research would be a full GW skymap, spanning the entire history of the universe, perhaps low resolution, however much like the COBE satellite proved the inhomogeniety of the CMB, our research would be the first step towards proving or disproving

features within the GWB, as well as concretely proving its existence.

6 Self Reflection

Overall I feel the research and development of the thesis went rather well, however there are a few areas I felt I could have improved on. Firstly, I feel as though I put too much focus on the practical side and not enough attention on taking notes and documenting my work, this lead to my supervisor feeling as though I had not done enough work as it was difficult for me to demonstrate. In the future I would like to work on making myself more organized and better capable of presenting my findings and work, and I feel as though this thesis has been an excellent step in that direction. Focusing too much on the practical side also left me with less time than I would have liked to interpret the results I received, and to make the thesis look as good possible. However, this is another thing I could feel myself improving on towards the end, working more efficiently and using my time better. I feel that I was able to discuss everything I felt was important, and that I captured the overall "big picture" of the research. To conclude, if I had to redo this Thesis, I would have definitely made more of an effort to be more organized and to better document my working over the weeks in order to be able to work more efficiently, and I feel as though going through this research will definitely help me to overcome these shortcomings in my future works.

7 Acknowledgments

This work would not have been possible without help from my supervisors, Ronald Westra and Gideon Koekoek, both of whom provided invaluable insight and helped me grow through my time working with them and provided great assistance in Section 2. Further, I would like to thank my Mother, Mirjana Simič, for helping me push through my struggles and with the calculation of cost for our satellite in Section 5.1. I would also like to thank my Father Mark Bowen for helping me create and edit the associated video.

8 Appendix

Instead of including a more detailed appendix within this document, please find all code and more examples of the Sun's lensing effect on my GitHub here.

References

[1] Penzias, A. A., & Wilson, R. W. (1965). A Measurement of Excess Antenna Temperature at 4080 Mc/s. The Astrophysical Journal, 142, 419–421.

[2] Smoot, G. F., et al. (1992). Structure in the COBE differential microwave radiometer first-year maps. The Astrophysical Journal, 396, L1.

[3] Bennett, C. L., et al. (2003). The Microwave Anisotropy Probe (MAP) Mission. The Astrophysical Journal, 583(1), 1-23.

[4] Planck Collaboration. (2014). Planck 2013 results. I. Overview of products and scientific results - Planck Collaboration. Astronomy & Astrophysics, 571, A1.

[5] Guth, A. H. (1981). The Inflationary Universe: A Possible Solution to the Horizon and Flatness Problems. Physical Review D, 23(2), 347–356.

[6] Kamionkowski, M., Kosowsky, A., & Stebbins, A. (1997). A Probe of Primordial Gravity Waves and Vorticity. Physical Review Letters, 78(11), 2058–2061.

[7] Abbott, B.P., et al. (2016). Observation of Gravitational Waves from a Binary Black Hole Merger. Physical Review Letters, 116(6), 061102.

[8] Abbott, B. P., et al. (2016). GW150914: The Advanced LIGO Detectors in the Era of First Discoveries. Physical Review Letters, 116(13), 131103. DOI: 10.1103/PhysRevLett.116.131103

[9] Abbott, B.P., et al. (2016). GW150914: Implications for the Stochastic Gravitational-Wave Background from Binary Black Holes. Physical Review Letters, 116(13), 131102. DOI: 10.1103/PhysRevLett.116.131102

[10] Einstein, A. (1916). Näherungsweise Integration der Feldgleichungen der Gravitation. Sitzungsberichte der Königlich Preußischen Akademie der Wissenschaften Berlin, part 1, 688–696.

[11] Will, C. (2014). The Confrontation between General Relativity and Experiment. Living Reviews in Relativity, 17(1), 4. DOI: 10.12942/lrr-2014-4

[12] Planck Collaboration. (2016). Planck 2015 results. XIII. Cosmological parameters. Astronomy & Astrophysics, 594, A13. DOI: 10.1051/0004-6361/201525830

[13] Abbott, B.P., et al. (2017). GW170104: Observation of a 50-Solar-Mass Binary Black Hole Coalescence at Redshift 0.2. Physical Review Letters, 118(22), 221101. DOI: 10.1103/PhysRevLett.118.221101

[14] Hild, S., Chassande-Mottin, E., & Freise, A. (2011). Potential of space-based interferometers. Classical and Quantum Gravity, 28(9), 094013. DOI: 10.1088/0264-9381/28/9/094013

[15] Punturo, M., et al. (2010). The third generation of gravitational wave observatories and their science reach. Classical and Quantum Gravity, 27(8), 084007. DOI: 10.1088/0264-9381/27/8/084007

[16] McNamara, P., et al. (2016). LISA Pathfinder: the experiment and the route to LISA. Classical and Quantum Gravity, 33(5), 054001. DOI: 10.1088/0264-9381/33/5/054001

[17] Amaro-Seoane, P., et al. (2017). Laser Interferometer Space Antenna. arXiv preprint arXiv:1702.00786.

[18] Caprini, C., et al. (2016). Science with the space-based interferometer eLISA. II: Gravitational waves from cosmological phase transitions. Journal of Cosmology and Astroparticle Physics, 2016(04), 001. DOI: 10.1088/1475-7516/2016/04/001

[19] Einstein, A. (1936). Lens-like action of a star by the deviation of light in the gravitational field. Science, 84(2188), 506-507. DOI: 10.1126/science.84.2188.506

[20] Bartelmann, M., & Schneider, P. (2001). Weak gravitational lensing. Physics Reports, 340(4-5), 291-472. DOI: 10.1016/S0370-1573(00)00082-X

[21] Takahashi, R., & Nakamura, T. (2003). Wave effects in gravitational lensing of gravitational waves from chirping binaries. Astrophysical Journal, 595(2), 1039. DOI: 10.1086/377512

[22] Röver, C., Bizouard, M. A., Christensen, N., Dimmelmeier, H., Krishnan, B., & Pai, A. (2007). Estimating the parameters of coalescing compact binaries using ground-based gravitational-wave detectors: I. Physical models and population-based priors. Physical Review D, 75(6).

[23] Fraisse, A. A., Ringeval, C., Spergel, D. N., & Bouchet, F. R. (2008). Small-angle CMB temperature anisotropies induced by cosmic strings. Physical Review D, 78(4).

[24] Virbhadra, K. S., & Ellis, G. F. (2000). Schwarzschild black hole lensing. Physical Review D, 62(8).

[25] Schneider, P., Ehlers, J., & Falco, E. E. (1992). Gravitational lenses. Springer.

[26] Baron, D., & Poznanski, D. (2017). The weirdest SDSS galaxies: results from an outlier detection algorithm. Monthly Notices of the Royal Astronomical Society, 465(1), 453-467.

[27] George, D., & Huerta, E. A. (2018). Deep learning for real-time gravitational wave detection and parameter estimation: Results with advanced LIGO data. Physics Letters B, 778, 64-70.

[28] Larson, S. L., Hiscock, W. A., & Hellings, R. W. (2000). Sensitivity curves for spaceborne gravitational wave interferometers. Physical Review D, 62(6), 062001. doi:10.1103/PhysRevD.62.062001

[29] Stensrud, E., Valero, M. A., & Alsyouf, I. (2018). Cost estimation of low cost planetary missions. Acta Astronautica, 148, 294-306. doi:10.1016/j.actaastro.2018.05.040

[30] Webster, G., Brown, D., & Cantillo, L. (2012, August 6). NASA Mars Rover Begins Driving at Bradbury Landing. NASA. Retrieved from https://www.jpl.nasa.gov/news/nasa-mars-rover-begins-driving-at-bradbury-landing

[31] Jennrich, O. (2009). LISA: Unresolved galaxies, confusion noise and the optimal mission. Classical and Quantum Gravity, 26(9), 094002. doi:10.1088/0264-9381/26/9/094002

[32] Dufour, F., & Laskar, J. (2013). Computing the sensitivity functions for the gravitational wave detectors LISA and LISA pathfinder. Astronomy & Astrophysics, 551, A36. doi:10.1051/0004-6361/201220586

[33] Smith, A. (n.d.). Tolman–Oppenheimer–Volkoff (TOV) Stars. University of Texas. Retrieved from https://www.as.utexas.edu

[34] Amaro-Seoane, P., Andrews, J., Arca Sedda, M., Askar, A., Baghi, Q., Balasov, R., ... VignaGómez, A. (2023). Astrophysics with the Laser Interferometer Space Antenna. Living Reviews in Relativity, 26(1). https://doi.org/10.1007/s41114-022-00041-y

[35] Bartelmann, M. (2010). Gravitational lensing. Classical and Quantum Gravity, 27(23), 233001. https://doi.org/10.1088/0264-9381/27/23/233001

[36] Landis, G. A. (1998). Mission to the Gravitational Focus of the Sun: A Critical Analysis.

[37] Leitao, L., Megevand, A., & Sanchez, A. D. (2012). Gravitational waves from the electroweak phase transition. Journal of Cosmology and Astroparticle Physics, 2012(10), 024–024. https://doi.org/10.1088/1475-7516/2012/10/024

[38] Takahashi, R., & Nakamura, T. (2003). Wave effects in the gravitational lensing of gravitational waves from chirping binaries. The Astrophysical Journal, 595(2), 1039–1051. https://doi.org/10.1086/377430

[39] Turyshev, S. G., & Toth, V. T. (2017). Diffraction of electromagnetic waves in the gravitational field of the Sun. Physical Review D, 96(2). https://doi.org/10.1103/physrevd.96.024008

[40] Turyshev, S. G., & Toth, V. T. (2020). Image formation process with the solar gravitational lens. Physical Review D, 101(4). https://doi.org/10.1103/physrevd.101.044048

[41] Birrer, S.,& Amara, A. (2018). lenstronomy: Multi-purpose gravitational lensing software package. Physics of the Dark Universe, 22, 189-210.

[42] Turyshev, S. G., Shao, M., Toth, V. T., Friedman, L. D., Alkalai, L., Mawet, D., Shen, J., Swain, M. R., Zhou, H., Helvajian, H., Heinsheimer, T., Janson, S., Leszczynski, Z., McVey, J., Garber, D., Davoyan, A., Redfield, S., & Males, J. R. (2020). Direct Multipixel Imaging and Spectroscopy of an Exoplanet with a Solar Gravity Lens Mission. arXiv preprint arXiv:2002.11871.

[43] Utina, A., Amato, A., Arends, J., Arina, C., Baar, M. de, Baars, M., Baer, P., Bakel, N. van, Beaumont, W., Bertolini, A., Beuzekom, M. van, Biersteker, S., Binetti, A., Brake, H. J. M. ter, Bruno, G., Bryant, J., Bulten, H. J., Busch, L., Cebeci, P., ... Zhang, T. (2022). ETpathfinder: A cryogenic testbed for interferometric gravitational-wave detectors. Classical and Quantum Gravity, 39(21), 215008. https://doi.org/10.1088/1361-6382/ac8fdb

[44] Misner, C. W., Thorne, K. S., & Wheeler, J. A. (1973). Gravitation. W. H. Freeman and Company.

[45] Dyson, F. W., Eddington, A. S., & Davidson, C. (1920). A Determination of the Deflection of Light by the Sun's Gravitational Field, from Observations Made at the Total Eclipse of May 29, 1919. Philosophical Transactions of the Royal Society of London. Series A, Containing Papers of a Mathematical or Physical Character, 220, 291-333.

[46] Will, C. M. (2015). The 1919 measurement of the deflection of light. Classical and Quantum Gravity, 32(12), 124001. https://doi.org/10.1088/0264-9381/32/12/124001

[47] Kippenhahn, R., Weigert, A., & Weiss, A. (2012). Stellar Structure and Evolution (2nd ed.). Springer-Verlag.

[48] Oppenheimer, J. R.; Volkoff, G. M. (1939). "On Massive Neutron Cores". Physical Review. 55 (4): 374–381. Bibcode:1939PhRv...55..374O. doi:10.1103/PhysRev.55.374.

[49] LeCun, Y., Bengio, Y., & Hinton, G. (2015). Deep learning. Nature, 521(7553), 436–444. DOI: 10.1038/nature14539

[50] Goodfellow, I., Bengio, Y., & Courville, A. (2016). Deep Learning. MIT Press. http://www.deeplearningbook.org/

[51] Rumelhart, D. E., Hinton, G. E., & Williams, R. J. (1986). Learning representations by back-propagating errors. Nature, 323(6088), 533–536. DOI: 10.1038/323533a0

[52] Woodahl, B. (2008). Retrieved from http://woodahl.physics.iupui.edu/Astro105/PREVIOUSindex.html

[53] Agazie, G., Anumarlapudi, A., Archibald, A. M., Arzoumanian, Z., Baker, P. T., Bécsy, B., ... Young, O. (2023). The nanograv 15 yr data set: Evidence for a gravitational-wave background. The Astrophysical Journal Letters, 951(1). doi:10.3847/2041-8213/acdac6